Mixed Uranium Chloride Fluorides $UF_{6-n}Cl_n$ and Methoxyuranium Fluorides $UF_{6-n}(OCH_3)_n$: A Theoretical Study of Equilibrium Geometries, Vibrational Frequencies, and the Role of the f Orbitals

Georg Schreckenbach*,‡

Theoretical Division (MS B268) and Seaborg Institute for Transactinium Science, Los Alamos National Laboratory, Los Alamos, New Mexico 87545

Received September 3, 1999

The title compounds, the uranium (VI) fluoride chlorides ($UF_{6-n}Cl_n$, $n = 0-6$) and methoxyuranium (VI) fluorides [$UF_{6-n}(OCH_3)_n$, $n = 0-5$], have been studied using relativistic density functional theory. Applying the B3LYP hybrid functional and an effective core potential on uranium, equilibrium geometries have been calculated for these molecules. In addition, harmonic vibrational frequencies have been computed for the chloride fluorides. Calculated frequencies have been compared to experiment where possible. All experimentally observed bands have been assigned, based on these calculations. The average deviation between theoretical and experimental frequencies is 15.6 cm^{-1} for 23 experimental modes. Theory always underestimates the experimental frequencies. This can be explained by the calculated bond lengths that are somewhat too long. The electronic structure of the uranium (VI) chloride fluorides has been investigated using scalar relativistic calculations and the PW91 functional. Periodic trends in the role and bonding contribution of the uranium 5f orbitals are discussed.

Introduction

Uranium hexafluoride, UF_6, is perhaps the most extensively studied actinide molecule, both experimentally[1−10] and theoretically.[11−27] On the other hand, derivatives of UF_6 where the fluorine ligands are successively replaced by some other ligand L, $UF_{6-n}L_n$ ($n = 1-6$), have received much less attention so far.

The chlorine ligand, L = Cl, has been the subject of a solution study by Downs and Gardner[28] who were able to characterize all of the mixed compounds ($n = 0-5$) by ^{19}F NMR spectroscopy. Later, the same authors also studied the chemistry and the IR spectrum of UF_5Cl.[29] Maier and co-workers published an IR absorption spectroscopic investigation on the same series of compounds.[30] In their combined low-temperature solution spectrum, lines could be assigned to all members of the series, i.e., $n = 0-6$. The dichloro compound *cis*-UF_4Cl_2 had also been produced earlier by reacting UF_4 with Cl_2 in a solid argon matrix,[31] and some IR absorption bands had been observed as well. More recently, a similar experimental approach, but starting from UCl_4, led to the observation of *trans*- and *cis*-UF_2Cl_4, as well as of UCl_6.[32]

Ligands other than chlorine have also been studied. Thus, Cuellar and Marks[33] synthesized the methoxy derivatives of UF_6, $UF_{6-n}(OCH_3)_n$, $n = 0-6$. All members of the series could be observed in solution by ^1H and ^{19}F NMR spectroscopy. Two years earlier, Vergamini had reported[34] the synthesis of the first member of the same series, UF_5OCH_3. The hexamethoxy derivative, $U(OCH_3)_6$, has also been studied experimentally[35]

‡ Present address: Department of Computational Science and Engineering, CLRC Daresbury Laboratory, Daresbury, Warrington, Cheshire, U.K. WA4 4AD.

(1) Blinc, R.; Marinkovic, V.; Pirkmajer, E.; Zupancic, I. *J. Chem. Phys.* **1963**, *38*, 2474.
(2) Weinstock, B.; Goodman, G. L. *Adv. Chem. Phys.* **1965**, *9*, 169.
(3) Seip, H. M. *Acta Chem. Scand.* **1965**, *20*, 2698.
(4) Blinc, R.; Pirkmajer, E.; Slivnik, J.; Zupancic, I. *J. Chem. Phys.* **1966**, *45*, 1488.
(5) McDowell, R. S.; Asprey, L. B.; Paine, R. T. *J. Chem. Phys.* **1974**, *61*, 3571.
(6) Paine, R. T.; McDowell, R. S.; Asprey, L. B.; Jones, L. H. *J. Chem. Phys.* **1976**, *64*, 3081.
(7) Miller, J. C.; Allison, S. W.; Andrews, L. *J. Chem. Phys.* **1979**, *70*, 3524.
(8) Le Bail, H.; Chachaty, C.; Rigny, P.; Bougon, R. *J. Physique Lett.* **1983**, *44*, 1017.
(9) Zeer, E. P.; Falaleev, O. V.; Zobov, V. E. *Chem. Phys. Lett.* **1983**, *100*, 24.
(10) Armstrong, D. P.; Harkins, D. A.; Compton, R. N.; Ding, D. *J. Chem. Phys.* **1994**, *100*, 28.
(11) Hay, P. J.; Wadt, W. R.; Raffenetti, R. C.; Phillips, D. H. *J. Chem. Phys.* **1979**, *71*, 1767.
(12) Hay, P. J. *J. Chem. Phys.* **1983**, *79*, 5469.
(13) Larsson, S.; Tse, J. S.; Esquivel, J. L.; Kai, A. T. *Chem. Phys.* **1984**, *89*, 43.
(14) Larsson, S.; Pyykkö, P. *Chem. Phys.* **1986**, *101*, 355.
(15) Onoe, J.; Takeuchi, K.; Nakamatsu, H.; Mukoyama, T.; Sekine, R.; Adachi, H. *Chem. Phys. Lett.* **1992**, *196*, 636.
(16) Onoe, J.; Takeuchi, K.; Nakamatsu, H.; Mukoyama, T.; Sekine, R.; Kim, B. I.; Adachi, H. *J. Chem. Phys.* **1993**, *99*, 6810.
(17) Onoe, J.; Sekine, R.; Takeuchi, K.; Nakamatsu, H.; Mukoyama, T.; Adachi, H. *Chem. Phys. Lett.* **1994**, *217*, 61.
(18) de Jong, W. A.; Nieuwpoort, W. C. *Int. J. Quantum Chem.* **1996**, *58*, 203.
(19) Malli, G. L.; Styszynski, J. *J. Chem. Phys.* **1996**, *104*, 1012.
(20) Onoe, J. *J. Phys. Soc. Jpn.* **1997**, *66*, 2328.
(21) Beu, T. A.; Onoe, J.; Takeuchi, K. *J. Chem. Phys.* **1997**, *106*, 5910.
(22) Beu, T. A.; Onoe, J.; Takeuchi, K. *J. Chem. Phys.* **1998**, *109*, 8295.
(23) Hay, P. J.; Martin, R. L. *J. Chem. Phys.* **1998**, *109*, 3875.
(24) Gagliardi, L.; Willetts, A.; Skylaris, C.-K.; Handy, N. C.; Spencer, S.; Ioannou, A. G.; Simper, A. M. *J. Am. Chem. Soc.* **1998**, *120*, 11727.
(25) Dolg, M. In *Encyclopedia of Computational Chemistry*; Schleyer, P. R. v., Ed.; Wiley-Interscience: New York, 1998.
(26) Schreckenbach, G.; Hay, P. J.; Martin, R. L. *J. Comput. Chem.* **1999**, *20*, 70.
(27) Pepper, M.; Bursten, B. E. *Chem. Rev.* **1991**, *91*, 719.
(28) Downs, A. J.; Gardner, C. J. *J. Chem. Soc., Dalton Trans.* **1984**, 2127.
(29) Downs, A. J.; Gardner, C. J. *J. Chem. Soc., Dalton Trans.* **1986**, 1289.
(30) Maier, W. B., II; Beattie, W. H.; Holland, R. F. *J. Chem. Soc., Chem. Commun.* **1983**, 598.
(31) Kunze, K. R.; Hauge, R. H.; Margrave, J. L. *Inorg. Nucl. Chem. Lett.* **1979**, *15*, 65.
(32) Hunt, R. D.; Andrews, L.; Toth, L. M. *Radiochim. Acta* **1993**, *60*, 17.
(33) Cuellar, E., A.; Marks, T. J. *Inorg. Chem.* **1981**, *20*, 2129.
(34) Vergamini *J. Chem. Soc., Chem. Commun.* **1979**, 54.

10.1021/ic9910615 CCC: $19.00
Published on Web 03/02/2000

and theoretically.[36] In the theoretical study by Bursten et al.,[36] the simple X-alpha version of density functional theory (DFT) has been used for single-point calculations only. These investigations, as well as the $UF_{6-n}Cl_n$ studies of Maier et al.[30] had been motivated, among others, by the potential of such compounds to be employed for uranium isotope separation.

The theoretical study of actinide complexes has recently seen a renewed interest.[25−27,37−39] This interest is motivated by fundamental as well as practical interest. Fundamental interest arises for at least two principal reasons, first, because of the challenges that are inherent in such studies,[26,27] and second, because the possibility of f orbital involvement in bonding may lead to completely new bonding schemes as compared to the upper parts of the periodic table. For instance, sandwich compounds involving the $C_8H_8^{2-}$ ligand[39−41] are not known for transition metals. Practical interest is primarily due to the radioactivity of the actinide elements and the experimental difficulties arising thereof. This leaves room for theory to provide useful data to augment and enhance experimental studies.

In this paper, we have used density functional theory[42−46] (DFT) to determine the structures of the title compounds, $UF_{6-n}Cl_n$, $n = 0-6$, and $UF_{6-n}(OCH_3)_n$, $n = 0-5$. To the best of our knowledge, these compounds have never been studied by first-principle quantum mechanical approaches before (apart, of course, from UF_6; see above). We have also calculated the vibrational frequencies of the chloride fluorides (L = Cl) where at least some experimental data is available for comparison and validation of the methods. At the same time, we were able to assign all observed bands based on our calculations.

The optimized structures have been used to calculate ligand and metal NMR chemical shifts in these compounds using relativistic DFT methods.[47−53] However, such NMR studies are beyond the scope of this paper. Preliminary results of these studies have been published already,[54] and detailed results will be presented elsewhere.[55,56]

In this contribution, we have further studied the electronic structure of the fluoride chlorides. Particular emphasis has been put on the role of the uranium 5f orbitals. This emphasis has two major motivations. First, f contributions to the bonding are unique for the early actinides, as has been pointed out already. Second, magnetically induced occupied-virtual f to f transitions may become important for the NMR properties of these compounds, notably the chemical shifts.[54−56] The uranium 5f orbitals would be nonbonding and unoccupied in a simple ionic picture. Yet, considerable bonding contributions are found. We will discuss periodic trends along the fluoride chloride series.

Computational Details

All calculations have been carried out using density functional theory, DFT.[42−46] In the past decade or so, DFT has been recognized as a very efficient and accurate method for treating the effects of electron correlation. Thus, it is particularly powerful for large systems including metal complexes. According to earlier studies,[57] we chose the B3LYP hybrid functional[58−60] as the approximation to the exchange-correlation functional of DFT. For complete consistency, all other settings have also been chosen to be the same as in our earlier studies on uranium complexes.[26,57] These settings will briefly be described in the following.

It is well-known that the (approximate) inclusion of relativistic effects is essential for even a qualitative understanding of the f-block elements and their chemistry.[27,61] Scalar relativistic effects have been included by employing a relativistic effective core potential (ECP) for the uranium atom.[12,23] In the ECP chosen, the uranium core comprises all shells up to and including the $4f^{14}$ and $5d^{10}$ shells. This leaves the outer core $6s^2$ and $6p^6$ shells as well as the valence shells proper (5f, 6d, 7s, 7d; six electrons) to be treated explicitly. Spin−orbit relativistic effects are thought to be unimportant for the structures and vibrational frequencies[62] of the complexes at hand that are formally f^0. Thus, such effects have been neglected.

We apply the following basis sets, again in agreement with our earlier investigations.[26,57] On ligand atoms, the standard 6-31+G* basis set has been used, whereas the uranium atom is described by a general ECP valence basis set[12,23] in its completely uncontracted form. This combination has been shown to yield structures and energies that are reasonably close to convergence with respect to basis set size.[57]

Structures, harmonic vibrational frequencies, and IR intensities have been computed with the GAUSSIAN94 program package.[63] A locally modified version of GAUSSIAN94 has been used to calculate analytic first and second derivatives of the total energy with respect to nuclear displacement.[64] These derivatives are essential to optimize geometries and, in particular, to calculate the vibrational frequencies. Achieving convergence in the self-consistent solution of the Kohn−Sham equations is notoriously difficult for actinide complexes, even if the f levels are formally unoccupied. As before,[57] a procedure of "building the guess" has been applied successfully to deal with these problems.

For the fluoride chlorides, single-point scalar relativistic calculations at the optimized geometries have also been performed with the Amsterdam density functional code ADF.[65−71] One of the major

(35) Cuellar, E. A.; Miller, S. S.; Marks, T. J.; Weitz, E. *J. Am. Chem. Soc.* **1983**, *105*, 4580.
(36) Bursten, B. E.; Casarin, M.; Ellis, D. E.; Fragalà, I.; Marks, T. J. *Inorg. Chem.* **1986**, *35*, 1257.
(37) Denning, R. G. *Struct. Bonding (Berlin)* **1992**, *79*, 215.
(38) Kaltsoyannis, N. *J. Chem. Soc., Dalton Trans.* **1997**, 1.
(39) Dolg, M.; Fulde, P. *Chem.—Eur. J.* **1998**, *4*, 200.
(40) Streitwieser, A.; Müller-Westhof, U. *J. Am. Chem. Soc.* **1968**, *90*, 7364.
(41) Streitwieser, A. *Inorg. Chim. Acta* **1984**, *94*, 171.
(42) Hohenberg, P.; Kohn, W. *Phys. Rev.* **1964**, *136*, B864.
(43) Kohn, W.; Sham, L. J. *Phys. Rev.* **1965**, *140*, A1133.
(44) Parr, R. G.; Yang, W. *Density-Functional Theory of Atoms and Molecules*; Oxford University Press: New York, Oxford, 1989.
(45) Ziegler, T. *Chem. Rev.* **1991**, *91*, 651.
(46) Ziegler, T. *Can. J. Chem.* **1995**, *73*, 743.
(47) Schreckenbach, G.; Ziegler, T. *J. Phys. Chem.* **1995**, *99*, 606.
(48) Schreckenbach, G.; Ziegler, T. *Int. J. Quantum Chem.* **1996**, *60*, 753.
(49) Schreckenbach, G.; Dickson, R. M.; Ruiz-Morales, Y.; Ziegler, T. In *Chemical Applications of Density Functional Theory*; ACS Symposium Series 629; Laird, B. B., Ross, R. B., Ziegler, T., Ed.; American Chemical Society: Washington, DC, 1996; p 328.
(50) Schreckenbach, G.; Ziegler, T. *Int. J. Quantum Chem.* **1997**, *61*, 899.
(51) Schreckenbach, G.; Ziegler, T. *Theor. Chem. Acc.* **1998**, *99*, 71.
(52) Wolff, S. K.; Ziegler, T. *J. Chem. Phys.* **1998**, *109*, 895.
(53) Wolff, S. K.; Ziegler, T.; van Lenthe, E.; Baerends, E. J. *J. Chem. Phys.* **1999**, *110*, 7689.
(54) Schreckenbach, G.; Wolff, S. K.; Ziegler, T. In *Modelling NMR Chemical Shifts: Gaining Insight into Structure and Environment*; ACS Symposium Series 732; Facelli, J. C., de Dios, A., Ed.; American Chemical Society: Washington, DC, 1999; p 101.
(55) Schreckenbach, G.; Wolff, S. K.; Ziegler, T. *J. Am. Chem. Soc.*, in press.
(56) Schreckenbach, G. *J. Am. Chem. Soc.*, in press.
(57) Schreckenbach, G.; Hay, P. J.; Martin, R. L. *Inorg. Chem.* **1998**, *37*, 4442.
(58) Lee, C.; Yang, W.; Parr, R. G. *Phys. Rev. B* **1988**, *37*, 785.
(59) Becke, A. D. *J. Chem. Phys.* **1993**, *98*, 5648.
(60) Stephens, P. J.; Devlin, F. J.; Chabalowski, C. F.; Frisch, M. J. *J. Phys. Chem.* **1994**, *98*, 11623.
(61) Pyykkö, P. *Chem. Rev.* **1988**, *88*, 563.
(62) van Lenthe, E.; Snijders, J. G.; Baerends, E. J. *J. Chem. Phys.* **1996**, *105*, 6505.
(63) Frisch, M. J.; Trucks, G. W.; Schlegel, H. B.; Gill, P. M. W.; Johnson, B. G.; Robb, M. A.; Cheeseman, J. R.; Keith, T.; Petersson, G. A.; Montgomery, J. A.; Raghavachari, K.; Al-Laham, M. A.; Zakrzewski, V. G.; Ortiz, J. V.; Foresman, J. B.; Cioslowski, J.; Stefanov, B. B.; Nanayakkara, A.; Challacombe, M.; Peng, C. Y.; Ayala, P. Y.; Chen, W.; Wong, M. W.; Andres, J. L.; Replogle, E. S.; Gomperts, R.; Martin, R. L.; Fox, D. J.; Binkley, J. S.; Defrees, D. J.; Baker, J.; Stewart, J. P.; Head-Gordon, M.; Gonzalez, C.; Pople, J. A. *Gaussian 94*, revision E.1; Gaussian, Inc.: Pittsburgh, PA, 1995.
(64) Russo, T. V.; Martin, R. L.; Hay, P. J.; Rappé, A. K. *J. Chem. Phys.* **1995**, *102*, 9315.
(65) Baerends, E. J.; Ellis, D. E.; Ros, P. *Chem. Phys.* **1973**, *2*, 41.

advantages of ADF is that it is particularly powerful for an analysis of the calculated electronic structure and the molecular orbitals. Thus, we have used such ADF single point calculations to study bonding in the complexes as well as the frontier orbitals across the entire fluoride chloride series. As mentioned in the Introduction, one aspect of the latter is the role of the, formally unoccupied, f-orbitals.

Hybrid functionals such as B3LYP are not available in ADF. Hence, the ADF calculations have been based on the PW91 XC functional.[72] This functional has been found to yield good results for actinide complexes.[73] Scalar relativistic effects are included using the "quasi-relativistic" (QR) method[74,75] that employs a Pauli-Hamiltonian[76] for the valence orbitals and the frozen core approximation[65] for the core orbitals. All other settings[77] are also the same as have been used elsewhere.[26,54]

Results and Discussion

1. Optimized Geometries. Key geometry parameters for the optimized structures of $UF_{6-n}L_n$ complexes are given in Tables 1 and 2 for L = Cl and L = OCH_3, respectively. We have further presented perspectivic pictures of a few of the optimized structures in Figure 1. Cartesian coordinates for the complete optimized structures are also included as Supporting Information for such cases where the structure is not completely defined by the data in the tables.

To the best of our knowledge, experimental geometries are only known for UF_6 proper. The calculated bond length, 2.024 Å, is seen to be too long by about 0.02−0.03 Å as compared to the experimental numbers of 1.996(8) Å[2] and 1.999(3) Å,[3] respectively. A similar behavior, i.e., theoretical bond lengths that are somewhat too long as compared to experiment, has been found in other cases as well.[23,26,57,78] Hence, it is reasonable to assume that all the calculated bond lengths are overestimated to some extent. This is also corroborated by the vibrational frequencies of the chloride fluorides that were calculated at the equilibrium geometries; see below.

The only other experimental structure[36] pertinent to the given study has been determined for the $n = 6$ member of the methoxy series, $U(OCH_3)_6$. This molecule has not been considered here but its measured U−O bond length of 2.10 Å (mean value) compares favorably to the calculated values for the $n = 5$ molecule, $UF(OCH_3)_5$. In $UF(OCH_3)_5$, the calculated U−O bond

Table 1. Optimized Geometries of Uranium (VI) Chloride Fluorides, $UF_{6-n}Cl_n$, $n = 0-6$; Key Geometry Parameters (Bond Lengths in Angstroms, Angles in Degrees)

molecule	symmetry	parameter	value
UF_6	O_h	R_{U-F}	2.0245
UF_5Cl	C_{4v}	R_{U-F} (F trans to Cl)	2.0247
		R_{U-F} (F trans to F)	2.0228
		R_{U-Cl}	2.5050
		$\angle_{Cl-U-F}$	89.70
cis-UF_4Cl_2	C_{2v}	R_{U-F} (F trans to Cl)	2.0253
		R_{U-F} (F trans to F)	2.0195
		R_{U-Cl}	2.5033
trans-UF_4Cl_2	D_{4h}	R_{U-F}	2.0212
		R_{U-Cl}	2.5056
fac-UF_3Cl_3	C_{3v}	R_{U-F}	2.0216, 2.0220, 2.0220
	distorted[a]	R_{U-Cl}	2.5002, 2.5006, 2.5006
mer-UF_3Cl_3	C_{2v}	R_{U-F}	2.0216, 2.0182, 2.0182
		R_{U-Cl}	2.5005, 2.5035, 2.5035
cis-UF_2Cl_4	C_{2v}	R_{U-F}	2.0208
		R_{U-Cl} (Cl trans to F)	2.4981
		R_{U-Cl} (Cl trans to Cl)	2.5009
trans-UF_2Cl_4	D_{4h}	R_{U-F}	2.0149
		R_{U-Cl}	2.5009
$UFCl_5$	C_{4v}	R_{U-F}	2.0147
		R_{U-Cl} (Cl trans to F)	2.4938
		R_{U-Cl} (Cl trans to Cl)	2.4978
		$\angle_{F-U-Cl}$	90.01
UCl_6	O_h	R_{U-Cl}	2.4944

[a] The optimized structure does not possess any symmetry but appears to be close to C_3 symmetry.

Table 2. Optimized Geometries of Methoxy Uranium (VI) Fluorides, $UF_{6-n}(OCH_3)_n$, $n = 1-5$; Selected Geometry Parameters (Bond Lengths in Angstroms, Angles in Degrees)

molecule	parameter	value
$UF_5(OCH_3)$	R_{U-F} (F trans to OCH_3)	2.0344
	R_{U-F} (F trans to F)	2.0441, 2.0451, 2.0512, 2.0508
	R_{U-O}	2.0366
	$\angle_{U-O-C}$	135.50
cis-$UF_4(OCH_3)_2$	R_{U-F} (F trans to OCH_3)	2.0524, 2.0591
	R_{U-F} (F trans to F)	2.0718, 2.0716
	R_{U-O}	2.0557, 2.0552
	$\angle_{U-O-C}$	138.66, 138.83
trans-$UF_4(OCH_3)_2$	R_{U-F}	2.0701, 2.0695
(C_i symmetry)	R_{U-O}	2.0448
	$\angle_{U-O-C}$	134.12
fac-$UF_3(OCH_3)_3$	R_{U-F}	2.0724, 2.0723, 2.0722
	R_{U-O}	2.0710, 2.0707, 2.0710
	$\angle_{U-O-C}$	137.29, 137.18, 137.36
mer-$UF_3(OCH_3)_3$	R_{U-F} (F trans to OCH_3)	2.0756
	R_{U-F} (F trans to F)	2.0892, 2.0834
	R_{U-O} (O trans to F)	2.0744
	R_{U-O} (O trans to OCH_3)	2.0626, 2.0614
	$\angle_{U-O-C}$	135.09, 137.81, 134.84
cis-$UF_2(OCH_3)_4$	R_{U-F}	2.0864, 2.0909
	R_{U-O} (O trans to F)	2.0920, 2.0907
	R_{U-O} (O trans to OCH_3)	2.0763, 2.0747
	$\angle_{U-O-C}$	136.67, 134.90, 138.45, 139.33
trans-$UF_2(OCH_3)_4$	R_{U-F}	2.1029
	R_{U-O}	2.0802, 2.0811
	$\angle_{U-O-C}$	135.95, 135.66
$UF(OCH_3)_5$	R_{U-F}	2.1036
	R_{U-O} (O trans to F)	2.1075
	R_{U-O} (O trans to OCH_3)	2.0935, 2.0926, 2.0930, 2.0925
	$\angle_{U-O-C}$	139.63, 136.78, 137.18, 136.99, 135.71

(66) Baerends, E. J.; Ros, P. *Chem. Phys.* **1973**, *2*, 52.
(67) Baerends, E. J. Ph.D. Thesis, Vrije Universiteit, Amsterdam, The Netherlands, 1973.
(68) Krijn, J.; Baerends, E. J. *Fit Functions in the HFS Method*; Internal Report (in Dutch); Department of Theoretical Chemistry; Vrije Universiteit: Amsterdam, The Netherlands, 1984.
(69) te Velde, G.; Baerends, E. J. *J. Comput. Phys.* **1992**, *99*, 84.
(70) Fonseca Guerra, C.; Visser, O.; Snijders, J. G.; te Velde, G.; Baerends, E. J. In *Methods and Techniques in Computational Chemistry METECC-95*; Clementi, E., Corongiu, C., Ed.; STEF: Cagliari, Italy, 1995; p 305.
(71) *ADF, 2.3, Theoretical Chemistry*; Vrije Universiteit: Amsterdam, The Netherlands, 1997.
(72) Perdew, J.; Wang, Y. *Phys. Rev. B* **1992**, *45*, 13244.
(73) Li, J.; Bursten, B. E. *J. Am. Chem. Soc.* **1998**, *120*, 11456.
(74) Boerrigter, P. M.; Baerends, E. J.; Snijders, J. G. *Chem. Phys.* **1988**, *122*, 357.
(75) Ziegler, T.; Tschinke, V.; Baerends, E. J.; Snijders, J. G.; Ravenek, W. *J. Phys. Chem.* **1989**, *93*, 3050.
(76) Pauli, W. *Z. Phys.* **1927**, *43*, 601.
(77) The ADF standard basis sets IV (U) and V (all other nuclei) were used. These are Slater type basis sets of triple-ζ quality in the valence region. They are augmented by two (basis V) or one (basis IV) sets of polarization functions. The orbitals up to and including 1s (C, O, F), 2p (Cl), and 5d (U), respectively, were considered as core and kept frozen in molecular calculations.[65] The respective core density and potential were obtained from preceding four-component relativistic atomic density functional calculations. Valence orbitals are orthogonalized against all cores in the molecule.[65,70] This procedure ensures, at least approximately, the proper asymptotic behavior in the core region. A set of auxiliary s, p, d, f, and g STO functions, centered on all nuclei, is part of the ADF standard basis sets. It was employed to fit the electron density and to present the density-dependent Coulomb and XC potentials accurately in each SCF cycle.[68]
(78) Hay, P. J.; Martin, R. L.; Schreckenbach, G. *J. Phys. Chem. A*, submitted.

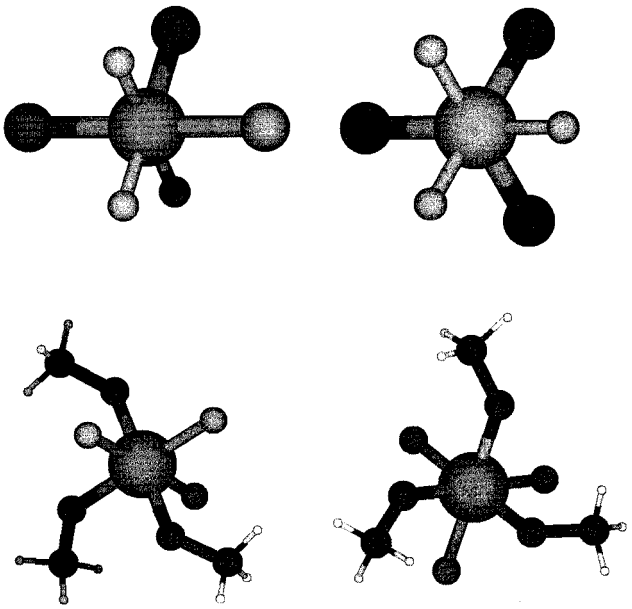

Figure 1. Optimized structures of *mer*- and *fac*-UF_3Cl_3 (upper row) and of *mer*- and *fac*-$UF_3(OCH_3)_3$ (lower row).

lengths are 2.09 Å for the four oxygens located cis to the fluorine atom and 2.11 Å for the reamining methoxy group, Table 2. Likewise, the mean experimental O−C distance in $U(OCH_3)_6$, 1.35 Å,[36] can be compared to the mean calculated O−C distance of 1.413 Å in $UF(OCH_3)_5$ (not shown in the table). Again, bond distances appear to be slightly overestimated by our calculations. It should be pointed out that the complete X-ray structure of the hexamethoxy uranium has never been published, due to crystallographic problems which led to very imprecise metrical parameters.[79]

It is likely that several energetically low-lying conformers exist for most of the methoxyuranium fluorides, $UF_{6-n}(OCH_3)_n$, in particular for the cases with n larger than one. Such conformers would differ mostly only by their arrangement of the various hydrogens, as well as by the relative orientation of the bent methoxy group(s) within the molecule. Hence, these are minor differences only, and we have made no attempt to locate more than one stable structure per compound, nor to check whether the given conformer is the global energy minimum in each case.

A few systematic trends are apparent upon inspection of Tables 1 and 2. First, let us compare the fluorine bond lengths for fluorine atoms that are situated trans to another fluorine and trans to a chlorine atom, respectively. It turns out that the former are always shorter by a small but significant amount for any given n, Table 1. The differences are 0.002 Å (UF_5Cl), 0.006 Å (*cis*-UF_4Cl_2), 0.003 Å (*mer*-UF_3Cl_3), and 0.006 Å (*cis*- vs *trans*-UF_2Cl_4).

There is a similar though somewhat less pronounced trend in the chlorine bond lengths. The bond lengths of chlorine atoms that are situated trans to a fluorine are somewhat shorter than for those trans to another chlorine atom. The differences are, in this case, 0.004 Å ($UFCl_5$), 0.003 Å (*cis*-UF_2Cl_4), 0.0004 Å (*mer*-UF_3Cl_3), and 0.0003 Å (*cis*- vs *trans*-UF_4Cl_2), Table 1.

These observed trends in the calculated structures should be due to the electronic structure of the systems studied. However, inspection of the calculations did not lead us to a simple explanation.

(79) Marks, T. J. Private communication, 1999.

Table 3. Energy Differences[a] (Relative Energies) between the $UF_{6-n}L_n$ Isomers ($n = 2-4$; L = Cl, OCH_3)

		energy difference[b]	
n	isomers	L = Cl	L = OCH_3
2	trans−cis	0.17	−3.70
3	mer−fac	0.11	−2.59
4	trans−cis	−0.06	−2.24

[a] GAUSSIAN94[63] based scalar relativistic ECP−B3LYP calculations. [b] In kcal/mol.

Turning now to the methoxy compounds, Table 2, the trend in the U−F bond lengths is just reversed. Fluorine atoms that are situated trans to another fluorine have, in this case, longer bond lengths than those trans to a methoxy group. The differences are larger than for the chloride case and amount to between 0.010 and 0.017 Å [$UF_5(OCH_3)$], 0.012 and 0.019 Å [*cis*-$UF_4(OCH_3)_2$], 0.008 and 0.014 Å [*mer*-$UF_3(OCH_3)_3$], and 0.012 and 0.017 Å [*cis*- vs *trans*-$UF_2(OCH_3)_4$], respectively. It is obvious that, in this case, steric effects dominate; a fluorine atom that is located trans to another fluorine atom has one more sterically demanding OCH_3 neighbor than a fluorine in the same molecule that is situated trans to one of the methoxy groups.

Another trend in the methoxy bond lengths is also easy to rationalize. Thus, we note from Table 2 that both, the U−F and the U−O bond lengths increase for decreasing numbers of fluorines. This trend is again readily rationalized based on steric considerations, taking into account the relatively large size of the methoxy groups.

2. Relative Energies of Isomers. The possibility of different conformations of the methoxyuranium fluorides, $UF_{6-n}(OCH_3)_n$, due to varying orientations of hydrogen atoms and methyl groups has been discussed in the preceding section. Apart from that, there are two distinct isomers each for the $UF_{6-n}L_n$ compounds for $n = 2$, 3, and 4. The relative energies of *cis*- vs *trans*-UF_4L_2 and UF_2L_4 as well as of *mer*- vs *fac*-UF_3L_3 (L = Cl, OCH_3) are given in Table 3.

The relative stability of the methoxy isomers seems to be completely determined by steric effects. We note that, in each case, the sterically less hindered isomer (trans, mer) is more stable by some 2−4 kcal/mol, according to our ECP-B3LYP calculations.

The energy differences are much smaller for the chloride fluorides, less than 0.2 kcal/mol in all cases, Table 3. Hence, both isomers would be thermally accessible at room temperature, provided that a suitable exchange pathway was available. Interestingly, and contrary to the methoxy case, *cis*-UF_4Cl_2 is found to be more stable than the trans isomer. Similarly, *fac*-UF_3Cl_3 is more stable than *mer*-UF_3Cl_3 by 0.1 kcal/mol. In these two cases, electronic factors appear to be determining the relative stability, whereas for the case of UF_2Cl_4, steric effects dominate, making the trans isomer very slightly more stable than the cis isomer at the given level of theory.

3. Frontier Orbitals of $UF_{6-n}Cl_n$, Periodic Trends. We have analyzed the electronic structure of the fluoride chloride series, $UF_{6-n}Cl_n$, $n = 0-6$. The electronic structure of UF_6 has been the subject of detailed studies[27] that can serve as the basis and starting point for the following discussion. Here, we will focus, in particular, on the role of the f orbitals. Moreover, we are interested in periodic trends across the series. It is normally only in actinide compounds that f orbitals can contribute significantly to bonding. As has been mentioned in the Introduction, the particular focus on the f orbitals is further motivated by their role for the calculated chemical shifts in these compounds.[54−56] The molecules in this study are all formally

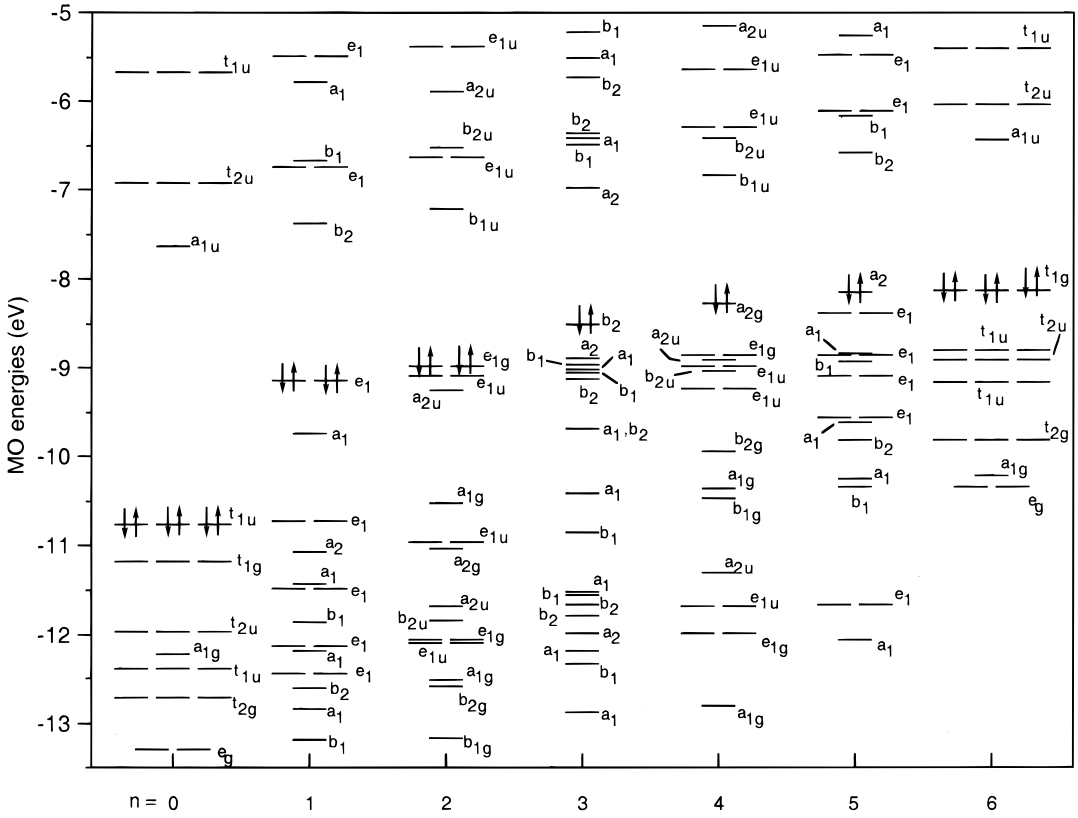

Figure 2. Calculated valence MO energies of $UF_{6-n}Cl_n$ molecules, $n = 0-6$, QR−PW91 calculations. The (fully occupied) HOMO is marked schematically in each case. The seven lowest virtual MOs are shown as well. The irreducible representations given refer to the O_h (UF_6, UCl_6), C_{4v} (UF_5Cl, $UFCl_5$), D_{4h} (*trans*-UF_4Cl_2, *trans*-UF_2Cl_4), and C_{2v} symmetries (*mer*-UF_3Cl_3), respectively.

Table 4. Selected MO Energies and MO Energy Differences (eV) of $UF_{6-n}Cl_n$ Molecules[a] ($n = 0-6$)

	HOMO energy		LUMO energy		HOMO−LUMO gap	
n[a]	QR-PW91[b]	ECP-B3LYP[c]	QR-PW91[b]	ECP-B3LYP[c]	QR-PW91[b]	ECP-B3LYP[c]
0	−10.752	−12.057	−7.628	−7.503	3.124	4.554
1	−9.136	−10.197	−7.369	−7.240	1.767	2.957
2	−8.978	−10.026	−7.206	−7.018	1.772	3.007
3	−8.511	−9.577	−6.972	−6.681	1.539	2.763
4	−8.271	−9.311	−6.833	−6.630	1.438	2.681
5	−8.147	−9.276	−6.574	−6.458	1.573	2.818
6	−8.126	−9.249	−6.437	−6.297	1.689	2.952

[a] Only the conformer with the highest symmetry has been included in cases where more than one conformer exists for a given n ($n = 2, 3, 4$). [b] ADF[65−71] based scalar relativistic (QR) PW91 calculations. [c] GAUSSIAN94[63] based scalar relativistic ECP−B3LYP calculations.

f^0 compounds. Hence, the seven 5f orbitals on uranium would be unoccupied in a simple ionic model.

Results for the methoxy series, $UF_{6-n}(OCH_3)_n$, are expected to be comparable to the analysis presented in this section. The lack of symmetry and the larger number of atoms and electrons would make the analysis more difficult in this case. Therefore, we have not extended the current analysis to these molecules.

The valence molecular orbitals of the $UF_{6-n}Cl_n$ molecules ($n = 0-6$) are presented graphically in Figure 2. The conformer with the highest symmetry has been chosen in cases where more than one conformer exists for a given n ($n = 2, 3, 4$). As pointed out before in the section Computational Details, we are mostly using scalar relativistic ADF calculations[65−71] and the PW91 XC functional[72] for the analysis that will be presented in this section. We have chosen this particular code and setting for two reasons. First, ADF allows for a detailed analysis of the results. The analysis makes full use of symmetry and is not available in this form elsewhere. Second, most of our relativistic NMR calculations are based on ADF and the PW91 functional.[54−56] Hence, a direct connection will be possible between the calculated ligand and metal chemical shifts[56] and the results of the following analysis.

The influence of different XC functionals on the calculated DFT MO energies have been studied in the literature for a limited number of molecules, including organic π-systems and polymers,[80,81] small molecules of first-row atoms,[82] and two iron complexes.[83] The experience to date[80−83] shows that occupied virtual energy gaps, including the HOMO−LUMO gap, are much larger with hybrid XC functionals (such as the B3LYP functional that has been used elsewhere in this article) as compared to GGA functionals[84] like PW91. We have collected the calculated HOMO and LUMO energies as well as the HOMO−LUMO gap of the $UF_{6-n}Cl_n$ molecules in Table 4. The

(80) Salzner, U.; Lagowski, J. B.; Pickup, P. G.; Poirier, R. A. *J. Comput. Chem.* **1997**, *18*, 1943.
(81) Salzner, U.; Pickup, P. G.; Poirier, R. A.; Lagowski, J. B. *J. Phys. Chem. A* **1998**, *102*, 2572.
(82) Politzer, P.; Abu-Awwad, F. *Theor. Chem. Acc.* **1998**, *99*, 83.
(83) Schreckenbach, G. *J. Chem. Phys.* **1999**, *110*, 11936.
(84) GGA stands for "generalized gradient approximation".

Table 5. Miscellaneous Properties of $UF_{6-n}Cl_n$ Molecules[a] ($n = 0-6$)

	U Mulliken charge[b]		U f Mulliken charge[b]		average f character of the six non-f_{xyz} virtuals[c,e] (%)	average position of occupied MOs with U 5f character[c,f] (eV)
n[a]	QR-PW91[c]	ECP-B3LYP[d]	QR-PW91[c]	ECP-B3LYP[d]		
0	4.75	2.78	−2.20	−2.40	82.0	−12.213
1	4.29	2.33	−2.27	−2.49	81.3	−11.425
2	3.94	1.87	−2.34	−2.58	80.8	−10.955
3	3.42	1.49	−2.41	−2.66	80.1	−10.371
4	3.05	1.07	−2.47	−2.75	79.5	−9.994
5	2.28	1.25	−2.52	−2.83	78.9	−9.449
6	1.85	0.94	−2.58	−2.91	78.5	−9.043

[a] Only the conformer with the highest symmetry has been included in cases where more than one conformer exists for a given n ($n = 2, 3, 4$). [b] In atomic units. [c] ADF[65-71] based scalar relativistic (QR) PW91 calculations. [d] GAUSSIAN94[63] based scalar relativistic ECP-B3LYP calculations. [e] The percentage f character has been calculated from the MO expansion coefficients into uranium based f-type basis functions. [f] Weighted average of the occupied MO energies, using degeneracy and percentage f character as the weighing factors, see the text.

table contains data for both, the ADF based QR-PW91 calculations and the Gaussian based ECP-B3LYP approach. Comparing the two sets of results, it turns out that the aforementioned conclusions can be extended to the uranium compounds at hand. Thus, introducing Hartree−Fock exchange (B3LYP functional) into pure DFT (PW91) leads to a strong stabilization of the HOMO, a slight destabilization of the LUMO, and consequently a large increase of the gap. Very similar effects have been seen before in the lower parts of the periodic table.[80-83]

On the other hand, the relative ordering and composition of the frontier MOs are much less influenced by the particular choice of XC functional. This is exemplified in Table 4 by the trends in the HOMO−LUMO gap along the fluoride chloride series. It is further supported by a direct comparison of the QR-PW91 and ECP-B3LYP calculations. Such a comparison shows that the overall MO picture is very similar, and the relative order of the frontier MOs differs in only few cases. Here, we are primarily interested in the position, relative energies, and f character of the valence MOs. Hence, we can use the combination of ADF calculations and the PW91 functional to study periodic trends across the uranium fluoride chloride series.

We have included valence orbitals only into Figure 2. The next lower occupied orbitals are found, in each case, below −20 eV (QR-PW91 calculations). Hence, they are semicore or core levels levels and will not be considered any further.

The seven lowest virtual MOs are shown as well. They are, in each case, the uranium 5f levels. As already mentioned, these levels are formally nonbonding. Yet, with the exception of the lowest unoccupied MO (LUMO), they contain a considerable degree of ligand admixture also (see below). Above the seven f levels, there is another sizable energy separation to the next higher virtual MOs. On the basis of the QR-PW91 calculations, this gap amounts to between 4.5 eV (UF_6) and 2.7 eV (*trans*-UF_2Cl_4).

Periodic trends can be recognized across the series. Let us start with the LUMO. It turns out that the LUMO is, in every case, a pure uranium f-orbital, namely, the f_{xyz}. Its symmetry properties are such that it cannot mix with any ligand combination for the molecules studied. For instance, in UF_6 and UCl_6 (O_h symmetry), it belongs to the a_{2u} irreducible representation. The energy of the f_{xyz} LUMO is increasing monotonically with increasing number of chlorine ligands, Table 4 and Figure 2. One can rationalize this trend by noting the increasing amount of electronic density at the uranium center. An indication for this is the Mulliken population analysis, Table 5. It has been noted that Mulliken charges are highly dependent on the basis set and are thus not the best representation of the effective nuclear charge. Yet, trends can nevertheless be studied. We have included into the table calculated uranium charges that were obtained from ADF[65-71] based QR-PW91 calculations[72,74,75] and from GAUSSIAN94[63] based ECP-B3LYP calculations,[12,23,58-60] respectively. As expected, the two sets of data differ markedly. Nevertheless, these charges can give a good indication of trends as, for example, for the given case of the $UF_{6-n}Cl_n$ molecules ($n = 0-6$), Table 5. The (positive) nuclear charge at the uranium center is decreasing with decreasing number of very electronegative fluorine ligands, from 4.8 au for UF_6 to 1.8 au for UCl_6 (ADF-PW91 calculations). The trend is the same for the ECP-B3LYP calculations where the charge changes less dramatically from 2.8 au (UF_6) to 0.9 au (UCl_6), Table 5. Clearly, the uranium nucleus becomes more effectively shielded along the series, and the (virtual) f orbitals experience a diminished nuclear attraction. This, in turn, results in the observed trend for the LUMO energies, Figure 2.

The six remaining f-type virtual orbitals are symmetry allowed to mix with ligand orbitals in each case. Indeed, all of them contain considerable ligand character. Being virtual orbitals, they are antibonding combinations of metal based f orbitals and corresponding ligand combinations. This slight antibonding character leads to higher MO energies as compared to the LUMO that is a pure, nonbonding f orbital, Figure 2. The average percentage f character of the six higher f-type virtuals has been included into Table 5. It is interesting that this f character decreases across the series, from 82.0% for UF_6 ($n = 0$) down to 78.5% for UCl_6 ($n = 6$). Thus, as the f character of these virtual MOs decreases, the f character of the corresponding occupied MOs must increase accordingly. These occupied MOs are bonding combinations of metal and ligand MOs. Hence, the bonding contribution of the uranium 5f orbitals increases with increasing number of chlorine ligands.

This increasing uranium 5f character of the occupied MOs can also be detected from the Mulliken population analysis. Thus, the Mulliken f charge at the uranium center increases from 2.20 electrons in UF_6 to 2.58 electrons in UCl_6, Table 5 (QR-PW91 calculations). Given a maximum possible f charge of 14 electrons, this corresponds to an f character of 15.7% in UF_6 and of 18.4% in UCl_6, in good qualitative agreement with the numbers obtained from the MO coefficients, Table 5. Similarly, the ECP-B3LYP calculations show the exact same trend, although the absolute numbers are somewhat larger in magnitude. The Mulliken f charges are, in this case, −2.40 au for UF_6 and −2.91 au for UCl_6, Table 5. These charges correspond to an increase in f character along the series from 17.1% (UF_6) to 20.8% (UCl_6), again in good qualitative agreement with the other numbers that were discussed before.

The increase in uranium 5f/ligand p mixing in going from UF_6 to UCl_6 can be understood from the relative electronegativities of the ligand nuclei. Thus, the lower electronegativity

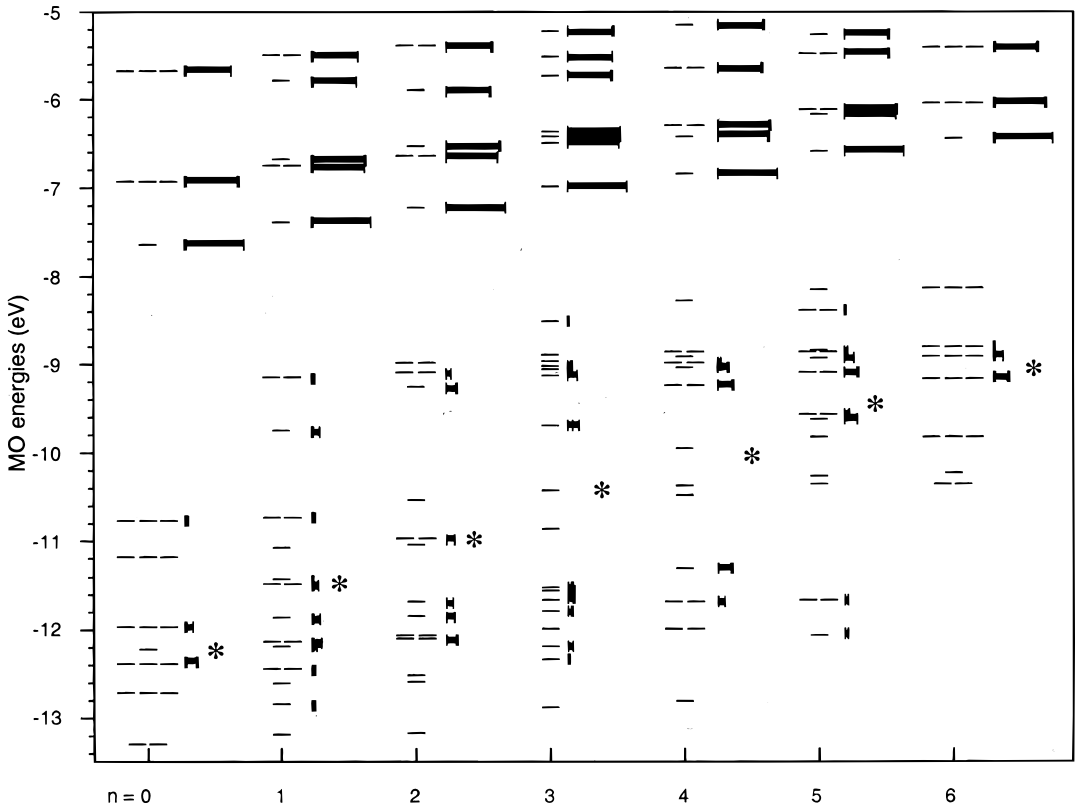

Figure 3. Valence MOs of $UF_{6-n}Cl_n$ molecules, $n = 0-6$. Calculated MO energies and percentage f character of valence MOs (solid black lines to the right of each individual MO diagram; the precentage f character has been calculated from the MO expansion coefficients into uranium based f-type basis functions). The LUMO is, in every case, a pure U $5f_{xyz}$ orbital. It therefore corresponds to 100% f character. Possible degeneracies have not been included into the precentage f character shown. Also shown for each molecule (marked by an asterisk $*$) is the average position of the occupied MOs with U 5f character; see Table 5 and the text.

of chlorine as compared to fluorine goes along with an increased radial extension and a less negative energy of the chlorine p atomic orbitals as compared to those of fluorine. Both factors facilitate the increased ligand−metal mixing, Table 5.

As mentioned in the Introduction, one particular aim of the current work is to lay the ground for the calculation and interpretation of NMR chemical shifts in the title compounds.[55,56] It is, by now, well-known that calculated chemical shifts as well as their periodic trends are determined by the magnetic coupling between specific occupied and virtual MOs. Often, but not always, these may include the HOMO or the LUMO. The strength of the coupling is proportional to certain "magnetic" (angular momentum) matrix elements and inversely proportional to the occupied-virtual energy separation. It is possible to analyze the magnetic coupling and its influence on the calculated chemical shifts in terms of pairs of canonical MOs.[47,51,52,83,85,86]

In diamagnetic actinide compounds, the magnetic coupling could, in principle, be based on 5f orbitals if there is an appreciable f contribution to the occupied (bonding) and virtual molecular orbitals. Hence, we are interested also in the amount and position of uranium 5f orbitals in the occupied molecular orbitals. We began this discussion in the previous paragraph (covering the amount f character in virtual and occupied MOs), and will continue in the following by analyzing periodic trends in the position of the f-containing bonding orbitals.

Naïvely, or as a first approximation, one could take the energy of the highest occupied molecular orbital (HOMO) and the HOMO−LUMO gap as measures for the position of the f-containing occupied MOs and the occupied-virtual f−f separation, respectively. The HOMO and LUMO energies as well as the HOMO−LUMO gap have been included into Table 4. It follows from this table and from Figure 2 that the HOMO−LUMO gap does not change smoothly along the $UF_{6-n}Cl_n$ series. Rather, the gap of about 3.1 eV in UF_6 (QR-PW91 calculations; 4.6 eV for ECP-B3LYP) is reduced considerably in UF_5Cl, and does not change strongly anymore for the rest of the series. This is, however, misleading with regards to the actual f contribution to bonding orbitals. It is appropriate to take a closer look.

This has been done in Figure 3 where we have repeated the MO energy diagrams of Figure 2 but have added the percentage f character for each MO as solid bars to the right of the respective MO diagram. As has been discussed already, the LUMO is, in every case, a pure U $5f_{xyz}$ orbital. Therefore, it corresponds to "100% f character", and its solid bar can serve as a quantitative scale to Figure 3. The data on which Figures 2 and 3 are based has been included as Supporting Information also.

We note from Figure 3 that the uranium 5f orbitals contribute to occupied MOs that are spread over a wide energy range, particularly for the intermediate members of the series ($n = 1-5$). Furthermore, it appears that the average position of these f-containing MOs changes much more smoothly along the series than the HOMO−LUMO gap. This can, indeed, be quantified. We have calculated a weighted average MO energy for the occupied MOs where the average has been weighted by the percentage f contribution (taken from the MO expansion coefficients) and by the degeneracy of the respective MO. The results have been included into Table 5 and Figure 3. The average position of the f orbitals in the occupied MOs increases monotonically in going from $n = 0$ (UF_6, −12.2 eV) to $n = 6$

Table 6. Vibrational Frequencies (cm^{-1}) and Calculated IR Intensities (in Brackets; KM/mol) of $UF_{6-n}Cl_n$ Molecules

UF_5Cl				*trans*-UF_4Cl_2			*cis*-UF_4Cl_2			
	frequency (IR intensity)				frequency (IR intensity)			frequency (IR intensity)		
label[a]	calcd	exp[f]	exp[g]	label[b]	calcd	exp[f]	label[c]	calcd	exp[f]	exp[i]
e	112 (0.1)			e_u	94 (0.1)		a_1	103 (0.0)		
b_2	138 (0)			b_{2u}	138 (0)		a_2	106 (0)		
e	156 (1.4)			e_g	141 (0)		b_2	126 (0.0)		
e	179 (7.5)			e_u	162 (5.9)		b_1	129 (1.1)		
a_1	180 (7.2)			a_{2u}	178 (3.8)		a_1	144 (0.1)		
b_1	180 (0)			b_{2g}	182 (0)		a_2	163 (0)		
a_1	321 (37.1)	332	334 (m)	a_{1g}	299 (0)		b_2	168 (4.5)		
b_2	514 (0)			a_{2u}	343 (105.4)		a_1	177 (1.0)		
a_1	550 (42.4)	564	566 (m)	b_{1g}	515 (0)		b_1	177 (5.7)		
e	606 (201.8)	618		a_{1g}	581 (0)		b_2	312 (43.5)		
a_1	619 (99.9)	646	649 (s)	e_u	606 (193.9)	618	a_1	331 (32.1)		
							a_1	535 (14.2)	548	
							b_2	568 (100.9)	578	581.3 (s)
							b_1	608 (194.0)	618	620.6 (vs)
							a_1	614 (146.4)	636	639.2 (s)

mer-UF_3Cl_3			*fac*-UF_3Cl_3[d]		*trans*-UF_2Cl_4			
	frequency (IR intensity)		frequency (IR intensity)			frequency (IR intensity)		
label[c]	calcd	exp[f]	calcd	exp[f]	label[b]	calcd	exp[f]	exp[h]
b_1	89 (0.0)		99 (0.0)		b_{2u}	81 (0)		
a_1	97 (0.0)		99 (0.0)		b_{2g}	90 (0)		
b_2	100 (0.0)		112 (0.1)		e_u	100 (0.0)		
b_1	125 (1.7)		117 (0.0)		a_{2u}	114 (1.4)		
b_2	139 (0.0)		138 (0.7)		e_g	149 (0)		
a_2	146 (0)		145 (0.9)		e_u	165 (1.9)		
a_1	163 (3.5)		170 (2.6)		b_{1g}	285 (0)		
b_2	172 (3.0)		171 (2.4)		a_{1g}	315 (0)		
b_1	176 (2.0)		182 (6.0)		e_u	343 (105.7)		350.8
a_1	295 (9.2)		312 (43.4)		a_{1g}	550 (0)		
a_1	326 (28.6)		313 (43.3)		a_{2u}	608 (177.5)	618	621.4
b_2	343 (106.0)		341 (29.0)					
a_1	538 (14.9)	555	567 (98.0)	579				
a_1	592 (105.8)	612	568 (97.8)	611				
b_1	607 (185.8)	618	612 (168.5)	631				

cis-UF_2Cl_4				$UFCl_5$			UCl_6			
	frequency (IR intensity)				frequency (IR intensity)			frequency (IR intensity)		
label[c]	calcd	exp[f]	exp[h]	label[a]	calcd	exp[f]	label[e]	calcd	exp[f]	exp[h]
a_1	91 (0.0)	(0.0)		b_2	85 (0)		t_{2u}	89 (0)		
b_2	94 (0.0)			e	95 (0.0)		t_{2g}	108 (0)		
a_2	99 (0)			b_1	101 (0)		t_{1u}	120 (0.2)		
b_1	109 (0.1)			e	116 (0.0)		e_g	287 (0)		
a_1	117 (0.2)			a_1	117 (0.7)		a_{1g}	333 (2.3)		
a_2	131 (0)			e	159 (1.2)		t_{1u}	342 (104.4)	354, 358	358.2
b_2	145 (1.7)			b_2	286 (0)					
b_1	156 (2.7)			a_1	303 (20.3)	322				
a_1	169 (3.0)			a_1	336 (18.2)					
a_1	294 (9.3)			e	343 (105.5)	358				
b_2	314 (42.6)			a_1	583 (105.9)	596				
a_1	339 (25.1)									
b_1	342 (106.1)		359.3							
b_2	568 (94.8)	579	579.2							
a_1	594 (130.6)	611	613.6							

[a] Symmetry label: C_{4v} symmetry. [b] Symmetry label, D_{4h} symmetry. [c] Symmetry label, C_{2v} symmetry. [d] Optimized structure has no apparent symmetry. [e] Symmetry label: O_h symmetry. [f] Reference 30, no experimental mode assignments. [g] Reference 29. [h] Reference 32, no experimental mode assignments. [i] Reference 31, no experimental mode assignments.

(UCl_6, −9.0 eV, QR-PW91 calculations). At the same time, the gap between occupied and virtual f-containing MOs is decreasing. Hence, one could expect increasing paramagnetic chemical shift contributions from f orbitals along the uranium fluoride chloride series.[55,56]

4. Harmonic Frequencies of $UF_{6-n}Cl_n$. We have also calculated the vibrational frequencies and infrared (IR) intensities for the mixed chloride fluoride compounds $UF_{6-n}Cl_n$, based on the harmonic approximation. As mentioned above, this has been carried out using the ECP-B3LYP approach[12,23,58−60] and the Gaussian program[63] including analytical second derivatives of the total energy with respect to nuclear displacement.[64] The results have been compiled in Table 6 where they are also compared to the available experimental data.[29−32] We have omitted UF_6 from the table. Previously, we have already compared and discussed the calculated and experimental vibrational frequencies of UF_6.[23,26] In these studies, the exactly same theoretical method, only with a slightly different basis set, had been employed. We have, at this point, not calculated the vibrational frequencies for the methoxy compounds where

Table 7. Average Deviation between Calculated and Experimental Vibrational Frequencies of $UF_{6-n}Cl_n$ Molecules

experimental reference	molecules included	number of modes included	average deviation (cm^{-1})
Kunze[31]	*cis*-UF_4Cl_2	3	17.5
Maier[30]	all $UF_{6-n}Cl_n$ species, $n = 0-6$[a]	23[a]	15.7
Downs[29]	UF_5Cl	3	19.7
Hunt[32]	*cis*-, trans-UF_2Cl_4, UCl_6	6	14.1

[a] Included here is the ν_3 mode of UF_6 with a calculated and observed[30] frequency of 607 and 618 cm^{-1}, respectively.

the lack of experimental data, combined with the large size of these molecules, does not justify the computational effort required.

For the molecules in Table 6, we see that there are three separate groups of harmonic frequencies. The lowest group, with calculated harmonic frequencies at about 180 cm^{-1} and below, comprises the various bending modes in the molecules. None of those frequencies has been observed to date. The next group of frequencies, calculated around 300−350 cm^{-1}, corresponds to U−Cl stretching modes. IR active modes out of this group have been observed in some cases (UF_5Cl, *trans*- and *cis*-UF_2Cl_4, $UFCl_5$, UCl_6). Finally, the highest vibrational frequencies, above 500 cm^{-1}, correspond to U−F stretching modes. All of these modes have been observed experimentally, provided they are not IR inactive by symmetry.

Experimental mode assignments are available only in one of the experimental papers[29] and only for three IR active modes of UF_5Cl. We see, for this case, that the calculations underestimate the measured experimental frequencies[29] with an average deviation of 19.7 cm^{-1}, Tables 6 and 7. The vibrational frequencies of the other compounds are underestimated to a similar degree. This confirms the assertion made earlier that the calculations overestimate the bond lengths: The vibrational frequencies were in all cases calculated at the optimized equilibrium geometry, and bond lengths that are somewhat too long should result in calculated stretching frequencies that are too small, Table 6.

Let us return for a moment to UF_5Cl and the measurements of Downs and Gardner,[29] Table 6. It is noteworthy that the mode with the highest calculated IR intensity (calculated frequency, 606 cm^{-1}; intensity, 201.8 KM/mol) has not been resolved in these experiments. This point had been discussed by the authors themselves who also expected a strong band to occur in their spectrum near 620 cm^{-1}. Their experimental setup resulted in a mixture of UF_6 and UF_5Cl in solution. The anticipated 620 cm^{-1} UF_5Cl band was hidden by the intense absorption due to UF_6 in this region of the spectrum.

We have attempted to use our calculation to assign the experimentally observed vibrational frequencies for cases where experimental mode assignments are not available, Table 6. This can be done unambiguously for the symmetry allowed U−F stretching modes, since all of them have been observed by Maier et al.[30] Similarly, the few available experimental U−Cl stretching frequencies could also be assigned based on the calculated vibrational frequencies and IR intensities, Table 6. We note that the calculated frequencies are systematically too small by amounts similar to those in the case of UF_5Cl, Table 7. Thus, for the 23 modes observed by Maier et al.,[30] we find an average deviation of 15.6 cm^{-1}, where we have only included those modes that were actually assigned in the paper of Maier et al. (cf. the discussion below. The inclusion of four or five more U−Cl modes would not significantly alter this number.) Similarly, the six modes observed by Hunt et al.[32] yield an average deviation of 14.1 cm^{-1} for the three molecules *cis*-, *trans*-UF_2Cl_4 and UCl_6. Finally, the three cis-UF_4Cl_2 U−F stretching modes that were observed by Kunze et al.[31] give an average deviation between theory and experiment of 17.5 cm^{-1}, Table 7. Again, most of these deviations should be attributed to optimized bond lengths that are somewhat too long as compared to experiment.

One could, in principle, further improve the agreement between theory and experiment by applying an empirical uniform scaling factor to the calculated frequencies.[87−90] We will, however, refrain from doing so for two reasons. On one hand, such scaling factors have been optimized for organic molecules,[89,90] and it is not clear whether they are useful for actinide complexes also. On the other hand, agreement between theory and experiment is quite satisfactory already, as has been discussed before.

The U−F stretching frequencies of the *cis*-UF_4Cl_2 molecule are an interesting case, Table 6. Two separate sets of experiments are available for this molecule. Thus, Kunze et al.[31] observed bands at 581.3, 620.6, and 639.2 cm^{-1}. In addition, relative intensities are given qualitatively in this paper. The band at 620.6 cm^{-1} was found to be "very strong", whereas the other two bands are "strong". We have assigned these three bands to the highest three U−F stretching modes of b_2, b_1, and a_1 symmetries with calculated vibrational frequencies of 568, 608, and 614 cm^{-1}, respectively. The calculated intensities correspond nicely to the experimentally observed ones, Table 6. Our assignment is further supported by the experimental work of Maier et al.[30] who observed all four U−F stretching modes. The three highest experimental bands are within 3 wavenumbers from the values measured by Kunze et al., thus supporting our assignments as given in the table.

The observed U−Cl stretching bands for the UF_5Cl and UCl_6 molecules are another interesting case. For each of them, there should be only one such stretch that is IR active, Table 6. However, Maier et al.[30] observed two modes each, at 332 and 340 cm^{-1} for UF_5Cl, and at 354 and 358 cm^{-1} for UCl_6, respectively. (Only one of the two is given in the table for the former.) Similarly, Downs and Gardner[29] report two lines in this region of their UF_5Cl spectrum, at 334 and 342 cm^{-1}, respectively (N_2 matrix). We attribute the extra lines to isotope effects with the higher frequency being, in each case, due to ^{35}Cl and the lower frequency to ^{37}Cl. This view is shared by Downs and Gardner.[29] They were able to show that the experimental intensity ratio for UF_5Cl is approximately 3:1. It thus corresponds to the relative natural abundance of the two isotopes.

Maier et al.[30] observed in their IR spectrum strong features at 618 and 358 cm^{-1} that, in each case, "comprise bands of several species". For the former, the U−F stretch, they were able to find those species experimentally, principally by studying solutions at varying concentrations of reactants. The results have been included into Table 6. However, for the band at 358 cm^{-1}, only UCl_6 and $UFCl_5$ could be identified unambiguously. For those two molecules, the corresponding calculated frequencies (IR intensities) are 342 cm^{-1} (104.4 KM/Mol) and 343 cm^{-1}

(85) Ruiz-Morales, Y.; Schreckenbach, G.; Ziegler, T. *J. Phys. Chem.* **1996**, *100*, 3359.
(86) Ruiz-Morales, Y.; Schreckenbach, G.; Ziegler, T. *Organometallics* **1996**, *15*, 3920.
(87) Pulay, P.; Fogarasi, G.; Boggs, J. E. *J. Am. Chem. Soc.* **1979**, *101*, 2550.
(88) Pulay, P.; Fogarasi, G.; Pongor, G.; Boggs, J. E.; Vargha, A. *J. Am. Chem. Soc.* **1983**, *105*, 7037.
(89) Rauhut, G.; Pulay, P. *J. Phys. Chem.* **1995**, *99*, 3093.
(90) El-Azhary, A. A.; Suter, H. U. *J. Phys. Chem.* **1996**, *100*, 15056.

(105.5 KM/Mol), respectively. From a further inspection of the table, we find calculated modes with very similar intensities and harmonic frequencies also for *cis*- and *trans*-UF_2Cl_4, *mer*-UF_3Cl_3, and *trans*-UF_4Cl_2, Table 6. Hence, it is very likely that these four molecules contribute to the experimentally observed feature at 358 cm^{-1}. A fifth molecule, *fac*-UF_3Cl_3, has an IR-active band calculated at 341 cm^{-1} but with a lower intensity. Thus, it might also contribute.

A similar case is given by the experiments of Kunze et al.[31] for UF_4Cl_2. These authors observed three IR-active modes for this molecule, Table 6. From that, they concluded that they should have the cis conformer present in solution because it has a total of four IR-active U−F stretches (as compared to just one that is not symmetry forbidden for the trans conformer). They go on to conclude that[31] "no evidence has been found to support the presence of *trans*-UF_4Cl_2". However, upon inspection of Table 6 one notes that the symmetry allowed U−F band in the trans conformer has a frequency that is very close to the strongest mode in *cis*-UF_4Cl_2, 606 vs 608 cm^{-1} (calculated). Hence, we are tempted to propose that the reaction mixture of Kunze et al.[31] contained both conformers, in which case the strongest band observed (620.6 cm^{-1}) would be due to a superposition of the b_1 stretch of *cis*-UF_4Cl_2 and the e_u stretch of *trans*-UF_4Cl_2. This view is also supported by Maier et al.[30] who assigned their 618 cm^{-1} band to both conformers.

Conclusions

In this article, we have applied relativistic DFT to the study of uranium (VI) complexes. Once more, DFT turned out to be a reliable tool for the theoretical study of these heavy actinide complexes.[26] Indeed, DFT is one of very few, if not the only, theoretical methods that can be applied routinely to comparatively large actinide complexes such as the methoxy derivatives of UF_6 that were considered here. As has been pointed out before,[26,27,91] theoretical methods have to be capable of accurately describing both, relativity *and* electron correlation, to be useful for the theoretical study of actinide complexes. This can be achieved with modern DFT. Moreover, DFT is much more efficient computationally than correlated ab initio methods. This is particularly relevant for actinide systems where the number of electrons is inherently large, even when only valence electrons are considered explicitly as is done, for instance, in ECP schemes.

We have reported optimized geometries for uranium (VI) fluoride chlorides, $UF_{6-n}Cl_n$, $n = 0-6$, and for methoxyuranium (VI) fluorides, $UF_{6-n}(OCH_3)_n$, $n = 0-5$. Experimental bond lengths are available only for UF_6. The agreement between theory and experiment is satisfactory in this case although the bond length is slightly overestimated. Similar behavior has been observed before for other actinide systems.[23,26,57,78] The trend is also confirmed by the calculated harmonic vibrational frequencies of the fluoride chlorides. The vibrational frequencies are systematically underestimated in comparison to the available experimental data, Tables 6 and 7. Indirectly, this points to calculated bond lengths that are somewhat too long.

For the optimized geometries of the fluoride chlorides, it was always found that fluorine atoms situated trans to another fluorine had shorter bond lengths than atoms situated trans to a chlorine atom. The situation is just reversed for the methoxy compounds where steric repulsion appears to dominate over electronic factors. Here, fluorine atoms situated trans to another fluorine have longer bond lengths than those situated trans to a methoxy group.

Calculated vibrational frequencies for the fluoride chlorides have been compared to experiment where possible, and the agreement is satisfactory, despite the mentioned slight underestimation. To the best of our knowledge, no experimental frequencies have been reported yet for the mixed methoxy compounds. Therefore, we decided not to calculate these vibrational spectra at the current time.

We have also studied the electronic structure of the uranium fluoride chloride series, $UF_{6-n}Cl_n$, with particular focus on the uranium 5f orbitals. The uranium 5f orbitals are formally nonbonding in these f^0 complexes. However, it was found that only the LUMO is a pure f orbital (f_{xyz}). Its energy increases monotonically with increasing *n*. This can be easily understood by studying the charge on the uranium center. Successively replacing fluorine ligands by the less electronegative chlorines allows more electronic charge to be centered at the metal, Table 5, and the virtual f orbitals are more effectively shielded from the attractive nuclear charge. The other six virtual f orbitals show significant ligand character as well that is increasing with growing number of chlorine ligands, Table 5. Accordingly, the f contribution to occupied bonding orbitals must be increasing too. Furthermore, we found that the weighted average of the f-containing occupied is rising in energy along the series, bringing them closer to the virtual f orbitals, Table 5. This factor, along with the increasing amount of f character for increasing *n* will lead to larger paramagnetic chemical shift contributions for larger *n*.[54] The calculated chemical shifts of the fluoride chlorides and methoxyuranium fluorides will we the subject of future publications.[55,56]

We have compared calculated DFT MO energies for different model XC functionals. Comparing pure DFT (the PW91[72] GGA) with hybrid DFT (the B3LYP[58−60] functional), we find that the HOMO is strongly stablized by the hybrid functional in each case. This goes along with a slight destablization of the LUMO and consequently a considerable increase in the HOMO−LUMO gap, Table 4. Very similar observations had been made earlier for the lower part of the periodic table.[80−83] On the other hand, periodic trends along the series or the relative ordering of the MOs are much less sensitive to the particular choice of functional.

All calculations have been done based on the scalar relativistic approximation, i.e., spin−orbit effects have been neglected. While this is a good approximation for structures and vibrational frequencies,[62] spin−orbit will have a large influence on the ordering and composition of the MOs, by splitting certain degenerate orbitals. This has been discussed in detail for UF_6.[27] Nevertheless, the general conclusions regarding the f contributions as outlined above should be the same for the scalar and spin−orbit relativistic cases.

Acknowledgment. The author thanks P. Jeffrey Hay and Richard L. Martin for helpful discussions and encouragement and Harry J. Dewey for assistance regarding the experimental data. He further acknowledges funding from the Seaborg Institute for Transactinium Science and from the Laboratory Directed Research and Development program of the Los Alamos National Laboratory, operated by the University of California under contract to the U.S. Department of Energy (W-7405-ENG-36). The MOLDEN freeware program has been used to create Figure 1.

Supporting Information Available: Tables S1−S19 containing complete optimized geometries as well as the data used for the creation of Figures 2 and 3. This material is available free of charge via the Internet at http://pubs.acs.org.

(91) Hess, B. A. *Ber. Bunsen-Ges. Phys. Chem.* **1997**, *101*, 1.

IC9910615